Computers and Mathematics with Applications 66 (2013) 608–620

Contents lists available at ScienceDirect

Computers and Mathematics with Applications

journal homepage: www.elsevier.com/locate/camwa

Fractional differential equations and related exact mechanical models

Mario Di Paola [a,1], Francesco Paolo Pinnola [a,*], Massimiliano Zingales [a,b,c]

[a] Dipartimento di Ingegneria Civile Ambientale, Aerospaziale e dei Materiali (DICAM), Università degli Studi di Palermo, Viale delle Scienze, Ed. 8, 90128-Palermo, Italy

[b] Dipartimento di Biomeccanica e Biomateriali, Istituto Euro Mediterraneo di Scienza e Tecnologia (I.E.ME.S.T.), Via E. Amari 123, 90139-Palermo, Italy

[c] BioMechanics and BioMaterials laboratory (BM)^2-lab, Mediterranean Center of Human Health and Advanced Biotechnologies (MED-CHHAB), Viale delle Scienze, Ed. 18, 90128-Palermo, Italy

ARTICLE INFO

Keywords:
Mechanical systems
Power-law description
Fractional hereditary materials
Discretized models
Modal transformation

ABSTRACT

The aim of the paper is the description of fractional-order differential equations in terms of exact mechanical models. This result will be archived, in the paper, for the case of linear multiphase fractional hereditariness involving linear combinations of power-laws in relaxation/creep functions. The mechanical model corresponding to fractional-order differential equations is the extension of a recently introduced exact mechanical representation (Di Paola and Zingales (2012) [33] and Di Paola et al. (2012) [34]) of fractional-order integrals and derivatives. Some numerical applications have been reported in the paper to assess the capabilities of the model in terms of a peculiar arrangement of linear springs and dashpots.

1. Introduction

The use of differential equations with non-integer powers of the differentiation order, namely fractional differential equations [1–5], is nowadays accepted in many fields of physics and engineering [6–11]. Indeed as soon as different kinds of experimental tests as creep/relation set-ups, diffusion/advection measures, voltage/current observations among others, need power-law fitting of date [12,13], fractional-order operators are involved [14–19]. Fractional-order differential equations have been reported in more detail, i.e. in the context of heat conduction [20–22], of material hereditariness [14,15,23,24], of non-local mechanics [25], of control of dynamical system [4,26,27].

One of the main drawbacks in the use of fractional-operators has been related to the lack of a proper physical picture of this mathematical operator and, therefore, to the representation of the phenomena ruled by fractional differential equations.

In recent studies the authors introduced some mechanical pictures of the presence of fractional-order operators in non-local mechanics [28–30] as well as in the context of non-local heat transfer [31,32] and in hereditary materials [33,34]. The correspondence among fractional operators and mechanical, chemical or electric analogues has been investigated since the mid of the nineties of the last century. In this regard we mention, i.e. for fractional hereditariness, some studies by Bagley and Torvik [35,36], Schiessel et al. [37], Heymans and Bauwens [38] among others. Similar considerations hold for other fields of physics and engineering applications. In more detail in [33] a mechanical model of hereditariness corresponding,

* Corresponding author. Tel.: +39 3283268584.
E-mail addresses: mario.dipaola@unipa.it (M. Di Paola), francescopinnola@unipa.it, francescopaolopinnola@gmail.com (F.P. Pinnola), massimiliano.zingales@unipa.it (M. Zingales).
[1] Fax: +39 091 6568407.

0898-1221/$ – see front matter
http://dx.doi.org/10.1016/j.camwa.2013.03.012

exactly, to a fractional-order rheologic stress–strain relation with any real exponent $0 \leq \beta \leq 1$ has been proposed, whereas a numerical assessment has been reported in [34]. The mechanical model is represented by a massless plate resting on massless Newtonian fluid restrained by means of independent dashpots. The authors termed this rheological model as Elasto-Viscous (EV), as far as $0 \leq \beta \leq 1/2$, and the corresponding material as Elasto-Viscous one since the elastic phase prevails over the viscous one at the beginning of the load history. Instead $1/2 \leq \beta \leq 1$ the mechanical model is represented by a massless shear-type indefinite column resting on a bed of independent dashpots. In this case the authors termed Visco-Elastic (VE) this kind of materials since the viscous phase prevails on the elastic one.

In this paper the mechanical model describing fractional hereditary material will be used to solve the fractional differential equations involved in the analysis of multiphase fractional hereditary materials. Indeed, in this case the relaxation/creep functions involve linear combinations of power-laws with different exponents yielding a rheological description in terms of linear combination of Caputo's fractional derivatives. The presence of multiple order fractional differential operators will be related to a proper mechanical model that corresponds, exactly, to the original fractional differential equation. Discretization of the continuous models lead to a set of ordinary differential equations that may be easily solved by means of the proper tools of dynamical system. Some numerical applications will be reported to assess the validity of the models.

2. Multiphase fractional hereditary materials (FHM)

The time dependent behavior of viscoelastic material may be introduced starting from the so-called relaxation function $G(t)$ that is the stress history $\sigma(t)$ for an assigned strain $\gamma(t) = U(t)$ being $U(t)$ the unit step function. Alternatively viscoelastic material may be characterized by the creep function $J(t)$ namely the strain history for the assigned stress history $\sigma(t) = U(t)$. In virtue of the Boltzmann superposition principle the stress–strain relations is expressed as

$$\sigma(t) = G(t)\gamma(0) + \int_0^t G(t-\tau)d\gamma(\tau) = G(t)\gamma(0) + \int_0^t G(t-\tau)\dot{\gamma}(\tau)d\tau \tag{1}$$

or in its inverse form

$$\gamma(t) = J(t)\sigma(0) + \int_0^t J(t-\tau)d\sigma = J(t)\sigma(0) + \int_0^t J(t-\tau)\dot{\sigma}(\tau)d\tau \tag{2}$$

where $\gamma(0)$ and $\sigma(0)$ are the strain and the stress in $t = 0$, respectively.

In the remainder of the paper it is assumed, without loss of generality, that $\gamma(0) = 0, \sigma(0) = 0$. Creep and relaxation function are related to each other by the following relationship in the Laplace domain [39]:

$$\hat{G}(s)\hat{J}(s) = \frac{1}{s^2} \tag{3}$$

being $\hat{G}(s)$ and $\hat{J}(s)$ the Laplace transform of $G(t)$ and $J(t)$, respectively.

Let us now suppose that from experimental relaxation test $G(t)$ is well fitted by

$$G(t) = \sum_{j=1}^{m} \frac{C(\beta_j)}{\Gamma(1-\beta_j)} t^{-\beta_j}; \quad 0 \leq \beta_j \leq 1 \tag{4}$$

where $\Gamma(\cdot)$ is the Euler gamma function and $C(\beta_j)$, β_j are parameters depending on the material at hands. Introducing Eq. (4) in Eq. (1) we obtain

$$\sigma(t) = \sum_{j=1}^{m} \frac{C(\beta_j)}{\Gamma\left(1-\beta_j\right)} \int_0^t (t-\tau)^{-\beta_j}\, \dot{\gamma}(\tau)d\tau = \sum_{j=1}^{m} C(\beta_j) \left({}^{C}D_{0^+}^{\beta_j}\gamma\right)(t) \tag{5}$$

where $\left({}^{C}D_{0^+}^{\beta_j}\gamma\right)(t)$ is Caputo's fractional derivative of order β_j. In the case of $m = 1$ the creep function, according to Eq. (3), is readily found in the form

$$J(t) = \frac{1}{C(\beta_1)\Gamma(1-\beta_1)} t^{\beta_1}. \tag{6}$$

It follows that, by inserting Eq. (6) in Eq. (1), we get

$$\gamma(t) = \frac{1}{C(\beta_1)} \frac{1}{\Gamma\left(1-\beta_1\right)} \int_0^t (t-\tau)^{\beta_1}\dot{\sigma}(\tau)d\tau = \frac{1}{C(\beta_1)} \left(D_{0^+}^{-\beta_1}\sigma\right)(t) \tag{7}$$

where $\left(D_{0^+}^{-\beta_1}\cdot\right)(t)$ is the Riemann–Liouville fractional integral.

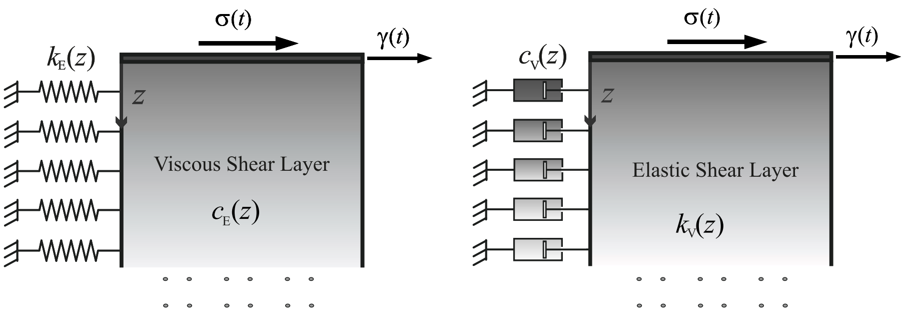

(a) Elasto-Viscous model ($0 \leq \beta \leq 1/2$). (b) Visco-Elastic model ($1/2 \leq \beta \leq 1$).

Fig. 1. Continuous fractional models.

The creep function for the more general case $m > 1$ in Eq. (4) is not so simple [40,41]. In order to illustrate difficulties emerging in the evaluation of the inverse relationship (5) for $m > 1$ the simple case is briefly illustrated. Let the relaxation function $G(t)$ give in the form

$$G(t) = G_\infty + \frac{C(\beta)}{\Gamma(1-\beta)} t^{-\beta} \tag{8}$$

in which the elastic phase is characterized by G_∞ and the viscous phase is represented by the second term in Eq. (8).

By performing Laplace transform and taking into account Eq. (3) the creep function corresponding to $G(t)$ expressed in Eq. (8) is found in the form [4,6,24]

$$J(t) = \frac{1}{G_\infty}\left[1 - E_\beta\left(-\frac{G_\infty}{C(\beta)}t^\beta\right)\right] = \frac{1}{G_\infty}\left[1 - \sum_{k=0}^{\infty}\frac{\left(-G_\infty/C(\beta)t^\beta\right)^k}{\Gamma(\beta k+1)}\right] = -\frac{1}{G_\infty}\sum_{k=1}^{\infty}\frac{\left(-G_\infty/C(\beta)t^\beta\right)^k}{\Gamma(\beta k+1)} \tag{9}$$

where $E_\beta(\cdot)$ is the one-parameter Mittag-Leffler function. By inserting Eq. (9) in Eq. (2) we get

$$\gamma(t) = \frac{1}{G_\infty}\left\{\sigma(t) + \sum_{k=0}^{\infty}\left[\left(\frac{G_\infty}{C(\beta)}\right)^{2k+1}\left(D_{0^+}^{-(2k+1)\beta}\sigma\right)(t) - \left(\frac{G_\infty}{C(\beta)}\right)^{2k}\left(D_{0^+}^{-2k\beta}\sigma\right)(t)\right]\right\}. \tag{10}$$

Inspection of Eq. (10) reveals that even in the simpler case in which the relaxation function assumes the form expressed in Eq. (8) the inverse relationship of Eq. (5) is very cumbersome and involves Riemann–Liouville fractional integrals of every order.

In the next section the extension of the mechanical model proposed by Di Paola and Zingales [33] is presented for the general case $m > 1$.

3. Exact mechanical model of multiphase viscoelastic systems

In this section the exact mechanical model of multiphase fractional viscoelastic system is presented. For the sake of completeness first the case $m = 1$ is treated and with this result the case $m > 1$ is really extended.

3.1. Exact mechanical model for $m = 1$

The stress–strain relation for the viscoelastic materials is expressed by fractional law in Eq. (7) or by its inverse expression

$$\sigma(t) = C(\beta_1)\left({}^C D_{0^+}^{\beta_1}\gamma\right)(t) \tag{11}$$

where $\left({}^C D_{0^+}^{\beta_1}\cdot\right)(t)$ is Caputo's fractional derivative.

In a previous paper [33] it has been shown that exact mechanical models of fractional viscoelasticity may be found for the two intervals of $\beta : 0 \leq \beta \leq 1/2$, $\beta : 1/2 \leq \beta \leq 1$. In the former case the material was labeled as Elasto-Viscous (EV) and the mechanical model is depicted in Fig. 1(a). While in the latter the material was labeled as Visco-Elastic (VE) and is depicted in Fig. 1(b).

The Elasto-Viscous case ($0 \leq \beta \leq 1/2$) is a massless indefinite viscous shear layer with a viscosity coefficient $c_E(z)$ resting on a bed of independent springs characterized by an elastic coefficient $k_E(z)$. In contrast the Visco-Elastic case

($1/2 \le \beta \le 1$) is a massless indefinite elastic shear layer characterized by a shear modulus $k_V(z)$ resting on a bed of independent viscous dashpots characterized by the viscosity coefficient $c_V(z)$. The subscripts E and V in $k(z)$ and $c(z)$ are introduced in order to distinguish the predominant behavior (E stands for Elasto-Viscous, while V stands for Visco-Elastic). Moreover we define G_0 and η_0 the reference values of the shear modulus and viscosity coefficient.

As soon as we assume

$$k_E(z) = \frac{G_0}{\Gamma(1+\alpha)} z^{-\alpha}; \qquad c_E(z) = \frac{\eta_0}{\Gamma(1-\alpha)} z^{-\alpha} \tag{12}$$

with $0 \le \alpha \le 1$ and $\beta = (1-\alpha)/2$, and

$$k_V(z) = \frac{G_0}{\Gamma(1-\alpha)} z^{-\alpha}; \qquad c_V(z) = \frac{\eta_0}{\Gamma(1+\alpha)} z^{-\alpha} \tag{13}$$

with $\beta = (1+\alpha)/2$, the stress $\sigma(t)$ at the upper lamina and $\gamma(t)$ the corresponding normalized displacement (that is the corresponding strain) revert to a fractional law expressed in Eq. (4) for $m = 1$, $\beta_1 = \beta$.

The governing equation for $0 \le \beta \le 1/2$ of the mechanical model depicted in Fig. 1(a) is

$$\frac{\partial}{\partial z}\left[c_E(z)\frac{\partial \dot{\gamma}(z,\ t)}{\partial z}\right] = k_E(z)\gamma(z,\ t). \tag{14}$$

The solution of the governing equation (14) in the Laplace domain involves the modified first and second kind Bessel functions; indeed we have

$$\hat{\gamma}(z,s) = z^{\beta}\left[B_{E1} I_\beta\left(\frac{z}{\sqrt{\tau_E(\alpha)s}}\right) + B_{E2} K_\beta\left(\frac{z}{\sqrt{\tau_E(\alpha)s}}\right)\right] \tag{15}$$

where $\hat{\gamma}(z,s)$ is the Laplace transform of $\gamma(z,t)$, while $I_\beta(\cdot)$ and $K_\beta(\cdot)$ are the modified first and second kind Bessel functions and $\tau_E(\alpha) = -\eta_0\Gamma(\alpha)/(\Gamma(-\alpha)G_0)$. The integration constants B_{E1} and B_{E2} are obtained by imposing the following boundary conditions:

$$\begin{cases} \lim\limits_{z\to 0} c_E(z)\dfrac{\partial\dot{\gamma}(z,t)}{\partial z} = \sigma(0,t) = \sigma(t), \\ \lim\limits_{z\to\infty} \gamma(z,t) = 0. \end{cases} \tag{16}$$

In this way the fractional constitutive law in Eq. (7) is obtained from the model depicted in Fig. 1(a) for $z \to 0$ (between the applied stress $\sigma(t)$ and the displacement of the top lamina $\gamma(0,t) = \gamma(t)$); indeed by performing the inverse Laplace transform with a simple algebraic manipulations, we get

$$\gamma(t) = \frac{1}{C_E(\beta)}\left(D_{0^+}^{-\beta}\sigma\right)(t) \tag{17}$$

where $C(\beta) = C_E(\beta)$ is defined as

$$C_E(\beta) = \frac{G_0\Gamma(\beta)2^{2\beta-1}}{\Gamma(2-2\beta)\Gamma(1-\beta)}\left(\tau_E(\alpha)\right)^{\beta}; \quad 0 \le \beta \le 1/2 \tag{18}$$

with $\beta = (1-\alpha)/2$.

The equilibrium equation of the continuous model depicted in Fig. 1(b) is written as

$$\frac{\partial}{\partial z}\left[k_V(z)\frac{\partial \gamma(z,\ t)}{\partial z}\right] = c_V(z)\dot{\gamma}(z,\ t) \tag{19}$$

and it represents the governing equation of exact VE model. Proceeding in a similar way to the previous case we obtain the following solution in Laplace domain:

$$\hat{\gamma}(z,s) = z^{\beta}\left[B_{V1} I_\beta\left(z\sqrt{\tau_E(\alpha)s}\right) + B_{V2} K_\beta\left(z\sqrt{\tau_E(\alpha)s}\right)\right] \tag{20}$$

where $\tau_V(\alpha) = -\eta_0\Gamma(-\alpha)/\Gamma(\alpha)G_0$. Eq. (20) can be solved by imposing the following boundary conditions:

$$\begin{cases} \lim\limits_{z\to 0} k_V(z)\dfrac{\partial\gamma(z,t)}{\partial z} = \sigma(0,t) = \sigma(t), \\ \lim\limits_{z\to\infty} \gamma(z,t) = 0. \end{cases} \tag{21}$$

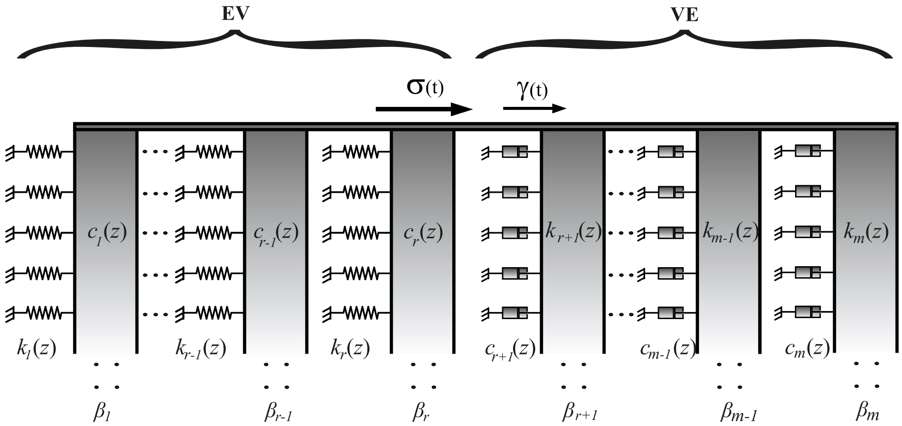

Fig. 2. Fractional multiphase viscoelastic material.

The solution of such differential equation for $z \to 0$ shows that the stress $\sigma(t)$ at the top is related to the normalized displacement $\gamma(t)$ by means of a fractional derivative of order $\beta = (1+\alpha)/2$. In fact we obtain

$$\gamma(t) = \frac{1}{C_V(\beta)} \left(D_{0^+}^{-\beta}\sigma\right)(t) \tag{22}$$

where the coefficient $C(\beta) = C_V(\beta)$ in the stress–strain relation reads

$$C_V(\beta) = \frac{G_0\,\Gamma(1-\beta)\,2^{1-2\beta}}{\Gamma(2-2\beta)\,\Gamma(\beta)} (\tau_V(\alpha))^{\beta}; \quad 1/2 \le \beta \le 1 \tag{23}$$

with $\beta = (1+\alpha)/2$.

We observed that by knowing G_0 and η_0 and for fixed value of β, both the coefficients $C_E(\beta)$ (for $0 \le \beta \le 1/2$) and $C_V(\beta)$ (for $1/2 \le \beta \le 1$) may be calculated according to Eqs. (18) and (23), respectively. Vice-versa if $C_E(\beta)$ (or $C_V(\beta)$) is known there exist ∞^1 possible choices of G_0 and η_0 that exactly restore $C_E(\beta)$ (or $C_V(\beta)$). In more detail, if we fix G_0, then for the EV case we get

$$\eta_0 = \left(\frac{C_E(\beta)\Gamma(2-2\beta)\Gamma(1-\beta)}{G_0^{1-\beta}\Gamma(\beta)2^{2\beta-1}}\right)^{1/\beta} \left(-\frac{\Gamma(-\alpha)}{\Gamma(\alpha)}\right); \quad 0 \le \beta \le 1/2 \tag{24}$$

while for the VE case

$$\eta_0 = \left(\frac{C_V(\beta)\Gamma(2-2\beta)\Gamma(\beta)}{G_0^{1-\beta}\Gamma(1-\beta)2^{1-2\beta}}\right)^{1/\beta} \left(-\frac{\Gamma(\alpha)}{\Gamma(-\alpha)}\right); \quad 1/2 \le \beta \le 2. \tag{25}$$

From Eqs. (24) and (25) we realize that provided η_0 is selected in Eq. (24) (for the EV case) or in Eq. (25) (for the VE case) the constitutive law $\sigma(t) = C(\beta)\left({}^{C}D_{0^+}^{\beta}\gamma\right)(t)$ is exactly restored on the top lamina of the two different models depicted in Fig. 1. Obviously both $\gamma(z,t)$ and $\sigma(z,t)$ depend on the selection of G_0 (or η_0) but the equilibrium on the top lamina does not depend on the particular choice of G_0 (or η_0) provided that G_0 and η_0 fulfill Eq. (24) or (Eq. (25)).

This issue will be reconsidered in the numerical examples.

3.2. Exact mechanical model for $m > 1$

With the previous results we now may find the mechanical model whose constitutive law is expressed in Eq. (5). We order β_j in such way that

$$0 \le \beta_1 < \beta_2 < \cdots \beta_r \le 1/2 \le \beta_{r+1} < \cdots < \beta_m \le 1. \tag{26}$$

For such a material characterized by coefficient β_j we have that the massless lamina on the top is sustained by r columns of massless Newtonian fluid resting on a bed of independent springs and $m-r$ shear type elastic columns resting on a bed of independent dashpots how it is described in Fig. 2.

At this stage we have r *EV* liquid columns sustained by external independent springs and $m-r$ shear type columns sustained by external dashpots. All these elements share a common displacement $\gamma(t)$ at the top of each column and then the load at the each lamina on the top has to be calibrated in such a way that the displacement on the top is equal for each column (compatibility condition) and $\sigma^{(j)}(t)$, the stress at each column, has to be such that $\sum_{j=1}^{m}\sigma^{(j)}(t)=\sigma(t)$ (equilibrium of the top lamina). So for this case the governing fractional differential equation representing stress–strain relation in multiphase materials becomes

$$C(\beta_1)\left({}^{C}D_{0^+}^{\beta_1}\gamma\right)(t)+\cdots+C(\beta_{r+1})\left({}^{C}D_{0^+}^{\beta_{r+1}}\gamma\right)(t)+C(\beta_r)\left({}^{C}D_{0^+}^{\beta_r}\gamma\right)(t)+\cdots+C(\beta_m)\left({}^{C}D_{0^+}^{\beta_m}\gamma\right)(t)=\sigma(t). \quad (27)$$

The inverse relationship of such equation, obtained by mathematical tools, involves a series of Riemann–Liouville fractional integrals of order greater than 1, how it is shown in Eq. (10) for the simple case of relaxation function expressed in Eq. (8). On the contrary with the mechanical model depicted in Fig. 2 the inverse relation may be obtained without losing the physical meaning ($0\le\beta_j\le 1$).

For example if we considered a fractional Kelvin–Voigt model in which we have a purely elastic phase in parallel with a fractional viscoelastic phase, we have a biphasic material; in fact $m=2$, $\beta_1=0$ and $1/2<\beta_2\le 1$. The elastic phase is characterized by elastic modulus G_∞ and the VE phase is characterized by coefficient $C(\beta_2)$ and exponent β_2; the relaxation function is given in Eq. (8) with $\beta_2=\beta$ and the stress–strain relation is expressed by

$$G_\infty\gamma(t)+C(\beta_2)\left({}^{C}D_{0^+}^{\beta_2}\gamma\right)(t)=\sigma(t). \quad (28)$$

By using the exact VE mechanical model previously described, the field of strain $\hat{\gamma}(z,s)$ in Laplace domain is identical to Eq. (20), but this equation must be solved by imposing different boundary conditions accounting for the response of the elastic phase, that is to say

$$\begin{cases}\lim\limits_{z\to 0}\left(G_\infty\gamma(z,t)-k_V(z)\dfrac{\partial\gamma(z,t)}{\partial z}\right)=\sigma(0,t)=\sigma(t),\\ \lim\limits_{z\to\infty}\gamma(z,t)=0\end{cases} \quad (29)$$

from Eq. (20) by imposing boundary conditions in Eq. (29) and for $z\to 0$ we obtain the exact Laplace transform of Eq. (28)

$$\hat{\gamma}(s)=\hat{\gamma}(0,s)=\lim_{z\to 0}\hat{\gamma}(z,s)=\hat{\sigma}(s)\frac{1}{C_V(\beta_2)s^{\beta_2}+G_\infty}. \quad (30)$$

It follows that the exact mechanical model for multiphase viscoelastic materials is that described in Fig. 2 and this enables us to properly discretize the mechanical model in order to get the inverse stress–strain relation. This issue will be reported in the next section.

4. Discretization of multiphase FHM

The mechanical representation of fractional order operators discussed in the previous section may be used to introduce a discretization scheme that corresponds to evaluate fractional derivative. How it has been shown in the previous section the multiphase FHM has a mechanical equivalence of r EV columns ($\beta\in[0,\ 1/2]$) and $m-r$ VE columns ($\beta\in[1/2,\ 1]$).

4.1. The discretized model of EV column

By introducing a discretization of the z-axis as $z_j=j\triangle z$ into the governing equation of the EV material in Eq. (14) yields a finite difference equation of the form

$$\frac{\triangle}{\triangle z}\left[c_E^{(i)}(z_j)\frac{\triangle\dot{\gamma}^{(i)}(z_j,\ t)}{\triangle z}\right]=k_E^{(i)}(z_j)\gamma^{(i)}(z_j,\ t);\quad i=1,2,\ldots,r \quad (31)$$

so that denoting $k_{Ej}^{(i)}=k_E^{(i)}(z_j)\triangle z$ and $c_{Ej}^{(i)}=c_E^{(i)}(z_j)/\triangle z$ the continuous model is discretized into a dynamical model constituted by massless shear layers, with horizontal degrees of freedom $\gamma^{(i)}(z_j,t)=\gamma_j^{(i)}(t)$, that are mutually interconnected by linear dashpots with viscosity coefficients $c_{Ej}^{(i)}$ resting on a bed of independent linear springs $k_{Ej}^{(i)}$.

The stiffness coefficient $k_{Ej}^{(i)}$ and the viscosity coefficient $c_{Ej}^{(i)}$ of the i-th column reads

$$k_{Ej}^{(i)}=\frac{G_0^{(i)}}{\Gamma(1+\alpha_i)}z_j^{-\alpha_i}\triangle z;\qquad c_{Ej}^{(i)}=\frac{\eta_0^{(i)}}{\Gamma(1-\alpha_i)}\frac{z_j^{-\alpha_i}}{\triangle z} \quad (32)$$

with $\alpha_i=1-2\beta_i$.

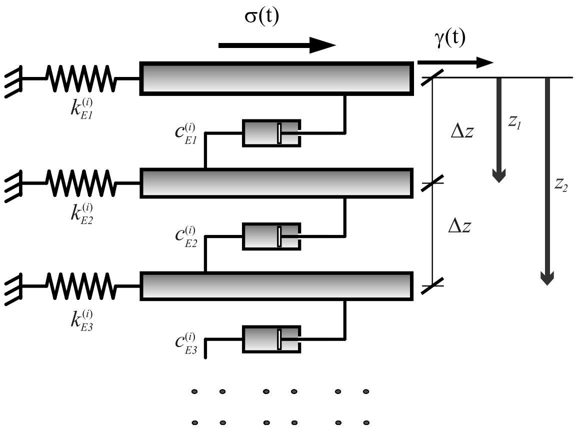

Fig. 3. Discretized counterpart of the continuous model Fig. 1(a): EV column.

The equilibrium equations of the generic shear-layer of the i-th model read

$$\begin{cases} k_{E1}^{(i)}\gamma_1^{(i)}(t) - c_{E1}^{(i)}\triangle\dot{\gamma}_1^{(i)}(t) = \sigma^{(i)}(t), \\ k_{Ej}^{(i)}\gamma_j^{(i)}(t) + c_{Ej-1}^{(i)}\triangle\dot{\gamma}_{j-1}(t) - c_{Ej}\triangle\dot{\gamma}_j^{(i)}(t) = 0, \quad j = 1, 2, \dots, \infty, \; i = 1, 2, \dots, r \end{cases} \tag{33}$$

where $\gamma_1^{(i)}(t) = \gamma(t)$ and $\triangle\dot{\gamma}_j^{(i)}(t) = \dot{\gamma}_{j+1}^{(i)}(t) - \dot{\gamma}_j^{(i)}(t)$. By inserting Eqs. (32) in Eqs. (33), at the limit as $\triangle z \to 0$, the discrete model reverts to Eq. (14). The discretized model presented in Fig. 3 represents a proper discretization of the continuous EV counterpart. As soon as z increase $\gamma^{(i)}(z,\ t)$ decay and $\lim_{z\to\infty}\gamma^{(i)}(z,t) = 0$ it follows that only a certain number, say n, of equilibrium equation may be accounted for the analysis. It follows that the system in Eq. (33) may be rewritten in the following compact form:

$$p_E^{(i)}\mathbf{A}^{(i)}\dot{\boldsymbol{\gamma}}^{(i)} + q_E^{(i)}\mathbf{B}^{(i)}\boldsymbol{\gamma}^{(i)} = \mathbf{v}\sigma^{(i)}(t) \tag{34}$$

where

$$p_E^{(i)} = \frac{\eta_0^{(i)}}{\Gamma(1-\alpha_i)}\triangle z^{-(1+\alpha_i)}; \qquad q_E^{(i)} = \frac{G_0^{(i)}}{\Gamma(1+\alpha_i)}\triangle z^{1-\alpha_i}. \tag{35}$$

The vectors $\boldsymbol{\gamma}^{(i)}$ and $\mathbf{v}$ in Eq. (34) are

$$\boldsymbol{\gamma}^{(i)^T} = \begin{bmatrix}\gamma_1^{(i)}(t) & \gamma_2^{(i)}(t) & \cdots & \gamma_n^{(i)}(t)\end{bmatrix}; \qquad \mathbf{v}^T = \begin{bmatrix}1 & 0 & 0 & \cdots & 0\end{bmatrix} \tag{36}$$

where the apex T means transpose. The matrices $\mathbf{A}^{(i)}$ and $\mathbf{B}^{(i)}$ are given as

$$\mathbf{A}^{(i)} = \begin{bmatrix} 1^{-\alpha_i} & -1^{-\alpha_i} & \cdots & 0 \\ -1^{-\alpha_i} & 1^{-\alpha_i}+2^{-\alpha_i} & \cdots & 0 \\ 0 & -2^{-\alpha_i} & \cdots & 0 \\ \vdots & \vdots & \ddots & \vdots \\ 0 & 0 & \cdots & (n-1)^{-\alpha_i}+n^{-\alpha_i} \end{bmatrix} \tag{37}$$

$$\mathbf{B}^{(i)} = \begin{bmatrix} 1^{-\alpha_i} & 0 & 0 & \cdots & 0 \\ 0 & 2^{-\alpha_i} & 0 & \cdots & 0 \\ 0 & 0 & 3^{-\alpha_i} & \cdots & 0 \\ \vdots & \vdots & \vdots & \ddots & \vdots \\ 0 & 0 & 0 & \cdots & n^{-\alpha_i} \end{bmatrix}. \tag{38}$$

The matrices $\mathbf{A}^{(i)}$ and $\mathbf{B}^{(i)}$ are symmetric and positive definite (in particular $\mathbf{B}^{(i)}$ is diagonal) and they may be easily constructed for an assigned value of α_i (depending on the derivative order β_i) and for a fixed truncation order n. Moreover Eq. (34) may now be easily integrated by using standard tools of dynamic analysis how it will be shown later on.

4.2. The discretized model of VE column

As the fractional order derivative of the s-th column ($r < s \le m$) is $\beta^{(s)} = \beta_V^{(s)} \in [1/2,\ 1]$ the mechanical description of the material is represented by the continuous model depicted in Fig. 4 and ruled by Eq. (19).

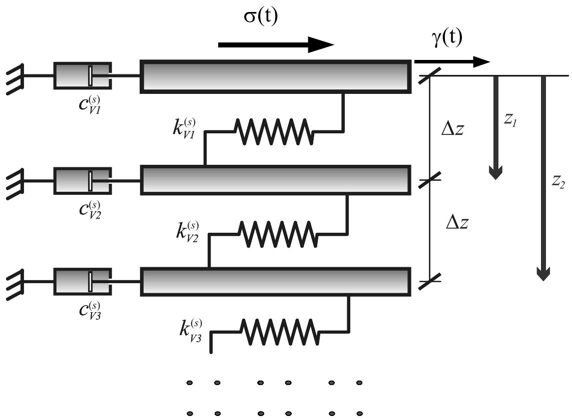

Fig. 4. Discretized counterpart of the continuous model Fig. 1(b): VE column.

By introducing a discretization of the z-axis in intervals $\triangle z$ in the governing equation of the VE materials in Eq. (19) yields a finite difference equation of the form

$$\frac{\triangle}{\triangle z}\left[k_V^{(s)}(z_j)\frac{\triangle\gamma^{(s)}(z_j,\ t)}{\triangle z}\right]=c_V^{(s)}(z_j)\dot{\gamma}^{(s)}(z_j,\ t);\quad s=r+1,r+2,\dots,m \tag{39}$$

that corresponds to a discretized mechanical representation of fractional derivatives. The mechanical model is represented by a set of massless shear layers with state variables $\gamma^{(s)}(z_j,\ t)=\gamma_j^{(s)}(t)$ that are mutually interconnected by linear springs with stiffness $k_{Vj}^{(s)}=k_V^{(s)}(z_j,\ t)/\triangle z$ resting on a bed of independent linear dashpots with viscosity coefficient $c_{Vj}^{(s)}=c_V^{(s)}(z_j,\ t)\triangle z$. Springs and dashpots are given as

$$k_{Vj}^{(s)}=\frac{G_0^{(s)}}{\Gamma(1-\alpha_s)}\frac{z_j^{-\alpha_s}}{\triangle z};\qquad c_{Vj}^{(s)}=\frac{\eta_0^{(s)}}{\Gamma(1+\alpha_s)}z_j^{-\alpha_s}\triangle z \tag{40}$$

with $\alpha_s=2\beta_s-1$.

The set of equilibrium equations reads

$$\begin{cases}c_{V1}^{(s)}\dot{\gamma}_1^{(s)}-k_{V1}^{(s)}\triangle\gamma_1^{(s)}=\sigma^{(s)}(t),\\ c_{Vj}^{(s)}\dot{\gamma}_j^{(s)}+k_{Vj-1}^{(s)}\triangle\gamma_{j-1}^{(s)}-k_{Vj}^{(s)}\triangle\gamma_j=0,\quad j=1,2,\dots,\infty,\ s=r+1,r+2,\dots,m,\end{cases} \tag{41}$$

so that, accounting for the contribution of the first n shear layers the differential equation system may be written as

$$p_V^{(s)}\mathbf{B}^{(s)}\dot{\boldsymbol{\gamma}}^{(s)}+q_V^{(s)}\mathbf{A}^{(s)}\boldsymbol{\gamma}^{(s)}=\mathbf{v}\sigma^{(s)}(t) \tag{42}$$

where

$$p_V^{(s)}=\frac{\eta_0^{(s)}}{\Gamma(1+\alpha_s)}\triangle z^{1-\alpha_s};\qquad q_V^{(s)}=\frac{G_0^{(s)}}{\Gamma(1-\alpha_s)}\triangle z^{-(1+\alpha_s)} \tag{43}$$

while $\boldsymbol{\gamma}^{(s)}$, $\mathbf{v}$ and the matrices $\mathbf{A}^{(s)}$ and $\mathbf{B}^{(s)}$ have already been defined in Section 4.1. The compatibility condition of the upper lamina reads $\gamma^{(s)}(0,t)=\gamma(t),\ \forall s: r+1\le s\le m$, while equilibrium equation reads $\sum_{s=r+1}^{m}\sigma^{(s)}=\sigma(t)$ being $\sigma(t)$ the external stress of the upper lamina.

5. Examples

The observations reported in the previous section lead to conclude that, whatever the class of FHM material is considered, the time-evolution of the system may be obtained by the introduction of a proper set of inner state variables, collected in the vector $\boldsymbol{\gamma}(t)$ and ruled by a set first-order linear differential equations. In this perspective the mechanical response of the FHM may be obtained in terms of the vector $\boldsymbol{\gamma}(t)$ by means of eigenvectors of the differential equations system reported in Eq. (33) for EV materials or in Eq. (41) for VE materials.

In this section three examples are reported, one is a fractional Kelvin–Voigt model with EV Spring-Pot ($\beta=\beta_E=0.4$), the second case consists in a Kelvin–Voigt model with VE Spring-pot ($\beta=\beta_V=0.6$), and then the last case is the fractional Kelvin–Voigt model with a critical value of $\beta=0.5$. The stiffness of the elastic spring is denoted with G_∞. The following numerical examples are obtained for $\sigma(t)=U(t)$.

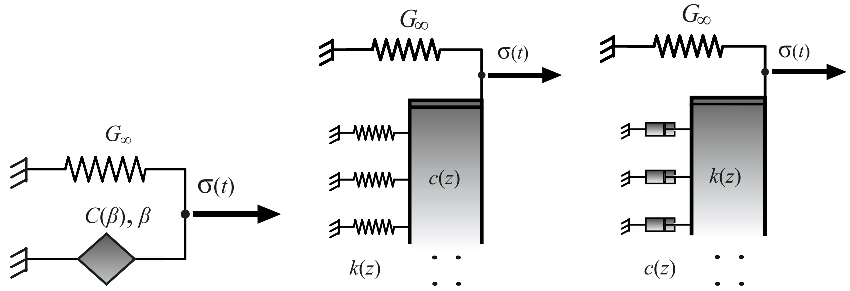

(a) Fractional Kelvin–Voigt model. (b) Kelvin–Voigt with EV phase. (c) Kelvin–Voigt with VE phase.

Fig. 5. Biphasic materials.

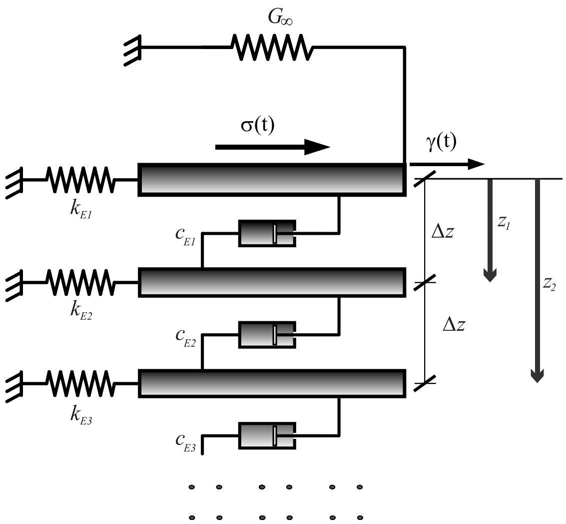

Fig. 6. Discretized fractional EV Kelvin–Voigt model.

5.1. The case of Kelvin–Voigt with EV Spring-Pot

In this section the fractional Kelvin–Voigt model depicted in Fig. 5 is investigated. In particular the Spring-Pot connected in parallel with the spring is of Elasto-Viscous type, for which the coefficient $\beta \in [0, 1/2]$. The discretized model is reported in Fig. 6. The governing equation is reported in Eq. (34). However, taking into account the presence of elastic spring connected in parallel with the EV Spring-Pot, the matrix $\mathbf{B} = \tilde{\mathbf{B}}$ becomes

$$\tilde{\mathbf{B}} = \begin{bmatrix} 1^{-\alpha} + \dfrac{G_\infty}{q_E} & 0 & 0 & \cdots & 0 \\ 0 & 2^{-\alpha} & 0 & \cdots & 0 \\ 0 & 0 & 3^{-\alpha} & \cdots & 0 \\ \vdots & \vdots & \vdots & \ddots & \vdots \\ 0 & 0 & 0 & \cdots & n^{-\alpha} \end{bmatrix}. \tag{44}$$

Therefore the differential equations system governing the equilibrium is rewritten in the following compact form:

$$p_E \mathbf{A}\dot{\boldsymbol{\gamma}} + q_E \tilde{\mathbf{B}}\boldsymbol{\gamma} = \mathbf{v}\sigma(t). \tag{45}$$

As customary we first solve the homogeneous case, that is as $\sigma(t) = 0$. We introduce a coordinate transformation in the form

$$\tilde{\mathbf{B}}^{1/2}\boldsymbol{\gamma} = \mathbf{x} \tag{46}$$

and premultiplying by $\tilde{\mathbf{B}}^{-1/2}$ a differential equation for the unknown vector $\mathbf{x}$ is obtained as

$$p_E \tilde{\mathbf{D}}\,\dot{\mathbf{x}} + q_E \mathbf{x} = \tilde{\mathbf{v}}\sigma(t) \tag{47}$$

where $\tilde{\mathbf{v}} = \tilde{\mathbf{B}}^{-1/2}\mathbf{v}$ and $\tilde{\mathbf{D}}$ is the dynamical matrix $\tilde{\mathbf{D}} = \tilde{\mathbf{B}}^{-1/2}\mathbf{A}\,\tilde{\mathbf{B}}^{-1/2}$ given as

$$\tilde{\mathbf{D}} = \begin{bmatrix} \dfrac{q_E}{q_E + G_\infty} & -\sqrt{\dfrac{q_E 2^\alpha}{q_E + G_\infty}} & \cdots & 0 \\ -\sqrt{\dfrac{q_E 2^\alpha}{q_E + G_\infty}} & 1 + \left(\dfrac{2}{1}\right)^\alpha & \cdots & 0 \\ 0 & -\left(\dfrac{3}{2}\right)^{\frac{\alpha}{2}} & \cdots & 0 \\ \vdots & \vdots & \ddots & \vdots \\ 0 & 0 & \cdots & 1 + \left(\dfrac{n}{n-1}\right)^\alpha \end{bmatrix} \tag{48}$$

where $\tilde{\mathbf{D}}$ is symmetric and positive definite and it may be obtained straightforwardly once n and α are fixed. Let $\tilde{\mathbf{\Phi}}$ be the modal matrix whose columns are the orthonormal eigenvectors of $\tilde{\mathbf{D}}$ that is

$$\tilde{\mathbf{\Phi}}^T \tilde{\mathbf{D}}\,\tilde{\mathbf{\Phi}} = \tilde{\boldsymbol{\Lambda}}; \qquad \tilde{\mathbf{\Phi}}^T \tilde{\mathbf{\Phi}} = \mathbf{I} \tag{49}$$

where $\mathbf{I}$ is the identity matrix and $\tilde{\boldsymbol{\Lambda}}$ is the diagonal matrix collecting the eigenvalues $\tilde{\lambda}_j > 0$ of $\tilde{\mathbf{D}}$.

In the following we order $\tilde{\lambda}_j$ in such a way that $\tilde{\lambda}_1 < \tilde{\lambda}_2 < \cdots < \tilde{\lambda}_n$. As we indicate $\mathbf{y}(t)$ the modal coordinate vector, defined as

$$\mathbf{x}(t) = \tilde{\mathbf{\Phi}}\,\mathbf{y}(t); \qquad \mathbf{y}(t) = \tilde{\mathbf{\Phi}}^T\,\mathbf{x}(t) \tag{50}$$

and substituting the Eq. (50) in Eq. (47) we obtain a decoupled set of differential equation in the following form:

$$p_E \tilde{\boldsymbol{\Lambda}}\,\dot{\mathbf{y}} + q_E \mathbf{y} = \bar{\mathbf{v}}\sigma(t) \tag{51}$$

where $\bar{\mathbf{v}} = \tilde{\mathbf{\Phi}}^T \tilde{\mathbf{v}} = \tilde{\mathbf{\Phi}}^T \tilde{\mathbf{B}}^{-1/2}\mathbf{v} = \tilde{\mathbf{\Phi}}^T \mathbf{v}$. The jth-equation of Eq. (51) reads

$$\dot{y}_j + \rho_j y_j = \frac{\tilde{\phi}_{1,j}}{p_E \tilde{\lambda}_j}\sigma(t); \quad j = 1, 2, 3, \ldots, n \tag{52}$$

where $\rho_j = q_E/(p_E \tilde{\lambda}_j) > 0$ and $\phi_{1,j}$ is the jth element of the first row of the matrix $\tilde{\mathbf{\Phi}}$. The solution of Eq. (52) is provided in the form

$$y_j(t) = y_j(0)\,e^{-\rho_j t} + \frac{\tilde{\phi}_{1,j}}{p_E \tilde{\lambda}_j}\int_0^t e^{-\rho_j(t-\tau)}\sigma(\tau)\,d\tau \tag{53}$$

where $y_j(0)$ is the jth component of the vector $\mathbf{y}(0)$ related to the vector of initial conditions $\boldsymbol{\gamma}(0)$ as

$$\mathbf{y}(0) = \tilde{\mathbf{\Phi}}^T \tilde{\mathbf{B}}^{1/2}\boldsymbol{\gamma}(0). \tag{54}$$

The solution of the differential equation system in Eq. (45) may be obtained as the modal vector $\mathbf{y}(t)$ has been evaluated by solving Eq. (53) with the aid of Eqs. (46) and (50) as

$$\boldsymbol{\gamma}(t) = \tilde{\mathbf{B}}^{-1/2}\tilde{\mathbf{\Phi}}\mathbf{y}(t). \tag{55}$$

We are interested to a relation among the shear stress and the normalized transverse displacement of the upper lamina (first element of vector $\boldsymbol{\gamma}(t)$) that is obtained as

$$\gamma(t) = \mathbf{v}^T \boldsymbol{\gamma}(t). \tag{56}$$

For quiescent system at $t = 0$ and forcing the model with $\sigma(t) = U(t)$ the solution $\gamma(t)$ obtained from Eq. (56) becomes

$$\gamma(t) = \sum_{j=1}^{n} \frac{\tilde{\phi}_{1,j}^2}{q_E + G_\infty}\left[1 - e^{-\rho_j t}\right]. \tag{57}$$

5.2. The case of Kelvin–Voigt with VE Spring-Pot

In this section the fractional Kelvin–Voigt is characterized for the presence of VE Spring-pot connected in parallel with elastic stiffness. The discretized model is depicted in Fig. 7. Modal analysis of the differential equations system representing

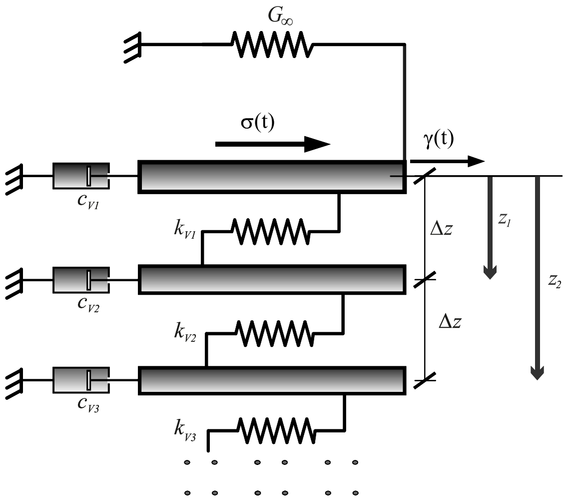

Fig. 7. Discretized fractional VE Kelvin–Voigt model.

the behavior of this fractional model is quite similar to the previous section. In this case the equilibrium equation system in the compact form becomes

$$p_V \mathbf{B}\dot{\boldsymbol{\gamma}} + q_V \hat{\mathbf{A}}\boldsymbol{\gamma} = \mathbf{v}\sigma(t) \tag{58}$$

where the matrix $\mathbf{B}$ is defined in Eq. (38), while the matrix $\hat{\mathbf{A}}$ becomes

$$\hat{\mathbf{A}} = \begin{bmatrix} 1^{-\alpha_i} + \dfrac{G_\infty}{q_V} & -1^{-\alpha_i} & \cdots & 0 \\ -1^{-\alpha_i} & 1^{-\alpha_i} + 2^{-\alpha_i} & \cdots & 0 \\ 0 & -2^{-\alpha_i} & \cdots & 0 \\ \vdots & \vdots & \ddots & \vdots \\ 0 & 0 & \cdots & (n-1)^{-\alpha_i} + n^{-\alpha_i} \end{bmatrix}. \tag{59}$$

In this case we substitute $\boldsymbol{\gamma} = \mathbf{B}^{-1/2}\mathbf{x}$ in Eq. (58) and we perform premultiplication by $\mathbf{B}^{-1/2}$:

$$p_V \dot{\mathbf{x}} + q_V \hat{\mathbf{D}}\,\mathbf{x} = \tilde{\mathbf{v}}\sigma(t) \tag{60}$$

where $\hat{\mathbf{D}} = \mathbf{B}^{-1/2}\hat{\mathbf{A}}\mathbf{B}^{-1/2}$ is the dynamical matrix defined as

$$\hat{\mathbf{D}} = \begin{bmatrix} \dfrac{q_V + G_\infty}{q_V} & -\left(\dfrac{2}{1}\right)^{\frac{\alpha}{2}} & \cdots & 0 \\ -\left(\dfrac{2}{1}\right)^{\frac{\alpha}{2}} & 1 + \left(\dfrac{2}{1}\right)^{\alpha} & \cdots & 0 \\ 0 & -\left(\dfrac{3}{2}\right)^{\frac{\alpha}{2}} & \cdots & 0 \\ \vdots & \vdots & \ddots & \vdots \\ 0 & 0 & \cdots & 1 + \left(\dfrac{n}{n-1}\right)^{\alpha} \end{bmatrix}. \tag{61}$$

The dynamical equilibrium equation in modal coordinate reads

$$p_V \dot{\mathbf{y}} + q_V \hat{\boldsymbol{\Lambda}}\,\mathbf{y} = \bar{\mathbf{v}}\sigma(t) \tag{62}$$

so that equilibrium of jth Kelvin–Voigt represented by Eq. (62) is given as

$$\delta_j \dot{y}_j + y_j = \frac{\hat{\phi}_{1,j}}{q_V \hat{\lambda}_j}\sigma(t); \quad j = 1, 2, 3, \ldots, n \tag{63}$$

where $\delta_j = p_V/(q_V \hat{\lambda}_j) > 0$.

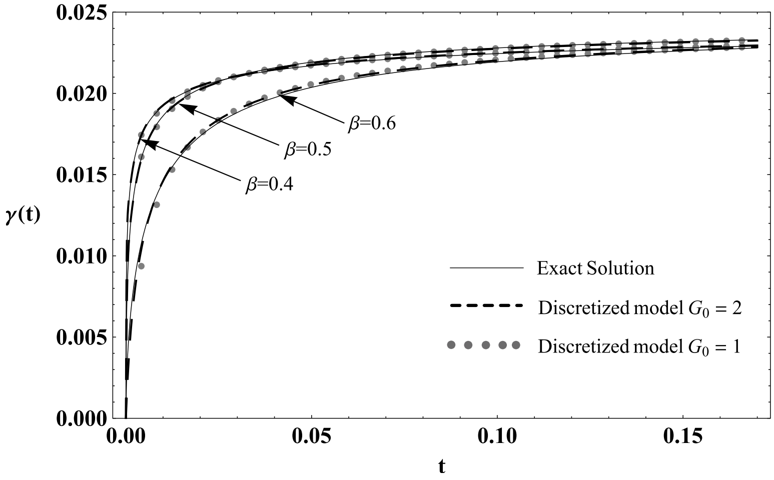

Fig. 8. Creep test of EV and VE Kelvin–Voigt models: comparison between the exact and approximate solution.

The solution in terms of modal coordinates are obtained in the integral form as

$$y_j(t) = y_j(0)\, e^{-t/\delta_j} + \frac{\hat{\phi}_{1,j}}{\delta_j\, q_V\, \hat{\lambda}_j} \int_0^t e^{-(t-\tau)/\delta_j} \sigma(\tau)\, d\tau. \tag{64}$$

The stress–strain relations between shear stress $\sigma(t)$ and normalized displacement $\gamma(t)$ may be obtained as in the previous section (see Eqs. (53) and (56)).

For the quiescent system at $t = 0$ and forcing the model with $\sigma(t) = U(t)$, the solution $\gamma(t)$ becomes

$$\gamma(t) = \sum_{j=1}^{n} \frac{\hat{\phi}_{1,j}^2}{q_V\, \hat{\lambda}_j} \left[1 - e^{-\frac{t}{\delta_j}}\right]. \tag{65}$$

The particular case in which the fractional Kelvin–Voigt model consists of perfect spring and Spring-Pot with $\beta = 0.5$ may be studied either starting from Eq. (57) or from Eq. (65).

In Fig. 8 the results for $\sigma(t) = U(t), G_0 = \eta_0 = 2,\ G_\infty = 20\,G_0,\ n = 750,\ \Delta z = 0.05$ and different values of $\beta = 0.4,\ 0.5,\ 0.6$ are contrasted with solution reported in Eq. (9) evaluated by *Mathematica*™.

Then the same example is performed by selecting $G_0 = 1$ and $\eta_0 = 2^{5/2}, 2^2, 2^{5/3}$ (respectively for the three different considered values of β) in this way $C(\beta)$ coalesce with that obtained by $G_0 = \eta_0 = 2$. The results of the two different models lead match the exact solution and then we conclude that whatever is the choice of G_0 provided η_0 is evaluated from Eq. (24) (for $0 \le \beta \le 1/2$) or from Eq. (25) (for $1/2 \le \beta \le 2$) the results in terms of displacement of the upper lamina do not change.

With these results we may conclude that the mechanical models with different values of G_0, but valuated each other in such a way that $C(\beta)$ remain constant leading to an identical stress–strain relation on the upper lamina.

6. Conclusions

One term fractional differential equations may be easily solved in terms of the known functions. Indeed the inverse relation of fractional hereditariness $\sigma(t) = C(\beta)\left({}^{C}D_{0^+}^{\beta}\gamma\right)(t)$ is readily found in the form $\gamma(t) = C(\beta)^{-1}\left(D_{0^+}^{-\beta}\sigma\right)(t)$.

A different scenario is involved as soon as we consider the case of multiple-term fractional differential equations whose solution is a hard task that has been solved in some specific case only. As an example, the inverse relationship of $\sigma(t) = \sum_{j=1}^{m} C(\beta_j)\left({}^{C}D_{0^+}^{\beta_j}\gamma\right)(t)$ is an open problem, unless $m = 2$ involving a convolution integral with two-parameter Mittag-Leffler kernel. As $m > 2$ no exact solutions exist and only numerical schemes, based on fractional difference methods and/or fractional finite element representation, may be found. Recently it has been shown that exact mechanical models of $\sigma(t) = C(\beta)\left({}^{C}D_{0^+}^{\beta}\gamma\right)(t)$ is represented by indefinite mechanical models constituted by massless fluid resting on a bed of springs ($0 \le \beta \le 1/2$) or by massless shear type column resting on a bed of dashpots ($1/2 \le \beta \le 1$). Springs and dashpots decrease with power-law related to the fractional order derivative β. With the aid of these mechanical models the problem of finding the strain history for an assigned stress history may be faced by using standard tools of dynamic analysis of mechanical systems. It is shown that in the general case $\sigma(t) = \sum_{j=1}^{m} C(\beta_j)\left({}^{C}D_{0^+}^{\beta_j}\gamma\right)(t)$ the mechanical model is massless plate interconnecting m columns r of them are fluids sustained by independent springs. While the remaining

$m - r$ are shear type columns resting on a bed of independent dashpots. Discretization of the two kind of columns and eigenanalysis of each column lead to a set of uncoupled, first-order differential equations that may be solved by classical methods of numerical analysis. Some numerical examples for the fractional Kelvin–Voigt model have been reported in the paper.

It is noted that the concepts explained in the paper may be extended for other cases that involve higher order fractional derivatives as for superconductors, visco-inertial systems, fractional diffusion equations, fractional controllers, and so on.

Acknowledgments

The authors are very grateful to research Grant No. PRIN2008, National Coordinator Professor A. Carpinteri. This financial support is gratefully acknowledged.

References

[1] K.B. Oldham, J. Spainer, The Fractional Calculus: Theory and Applications of Differentiation and Integration to Arbitrary Order, Academic Press, New York, 1974.
[2] K.S. Miller, B. Ross, An Introduction to the Fractional Calculus and Fractional Differential Equations, Wiley-InterScience, New York, 1993.
[3] G.S. Samko, A.A. Kilbas, O.I. Marichev, Fractional Integrals and Derivatives: Theory and Applications, Gordon and Breach, New York, NY, 1993.
[4] I. Podlubny, Fractional Differential Equations, Academic Press, San Diego, 1999.
[5] A.A. Kilbas, H.M. Srivastava, J.J. Trujillo, Theory and Applications of Fractional Differential Equations, Elsevier, Amsterdam, 2006.
[6] R. Hilfer, Application of Fractional Calculus in Physics, World Scientific, Singapore, 2000.
[7] V.E. Tarasov, Fractional Dynamics: Applications of Fractional Calculus to Dynamics of Particles, Fields and Media, Springer, 2010.
[8] R. Herrmann, Fractional Calculus An Introduction for Physicists, World Scientific Publishing Company, 2011.
[9] A.K. Golmankhaneh, Investigations in Dynamics: With Focus on Fractional Dynamics, Lap Lambert Academic Publishing, 2012.
[10] D. Baleanu, K. Diethelm, E. Scalas, J.J. Trujillo, Fractional Calculus Models and Numerical Methods, World Scientific Publishing Company, 2012.
[11] A.K. Golmankhaneh, A.M. Yengejeh, D. Baleanu, On the fractional Hamilton and Lagrange mechanics, International Journal of Theoretical Physics 51 (2012) 2909–2916.
[12] P.G. Nutting, A new general law of deformation, Journal of the Franklin Institute 191 (1921) 679–685.
[13] M. Di Paola, A. Pirrotta, A. Valenza, Visco-elastic behavior through fractional calculus: an easier method for best fitting experimental results, Mechanics of Materials 43 (2011) 799–806.
[14] G.W. Scott Blair, The role of psychophysics in rheology, Journal of Colloid Science 2 (1947) 21–32.
[15] G.L. Slonimsky, On the law of deformation of highly elastic polymeric bodies, Doklady Akademii Nauk SSSR 2 (1961) 343–346 (in Russian).
[16] R. Metzler, J. Klafter, The random walk's guide to anomalous diffusion: a fractional dynamics approach, Physics Reports 339 (2000) 1–77.
[17] A.V. Chechkin, V.Yu. Gonchar, R. Gorenflo, N. Korabel, I.M. Sokolov, Generalized fractional diffusion equations for accelerating subdiffusion and truncated Lévy flights, Physical Review E 78 (2008) 741–748.
[18] G.E. Carlson, C.A. Halijak, Approximation of fractional capacitors $(1/s)^{1/n}$ by a regular Newton process, IRE Transactions on Circuit Theory CT-11 (1964) 210–213.
[19] S. Westerlund, L. Ekstam, Capacitor theory, IEEE Transactions on Dielectrics and Electrical Insulation 1 (1994) 826–839.
[20] Y.Z. Povstenko, Thermoelasticity that uses fractional heat conduction equation, Journal of Mathematical Sciences 162 (2008) 296–305.
[21] H.H. Sherief, A.M.A. El-Sayed, A.M. Abd El-Latief, Fractional order theory of thermoelasticity, International Journal of Solids and Structures 47 (2010) 269–275.
[22] H.M. Youssef, E.A. Al-Lehaibi, Variational principle of fractional order generalized thermoelasticity, Applied Mathematics Letters 23 (2010) 1183–1187.
[23] M. Caputo, Elasticità e Dissipazione, Zanichelli, Bologna, 1969.
[24] F. Mainardi, Fractional Calculus and Waves in Linear Viscoelasticity, Imperial College Press, World Scientific, London, 2010.
[25] K.A. Lazopoulos, Non-local continuum mechanics and fractional calculus, Mechanics Research Communications 33 (2006) 75–757.
[26] S. Das, Functional Fractional Calculus for System Identification and Controls, Springer, 2010.
[27] D. Baleanu, Fractional Dynamics and Control, Springer, 2012.
[28] M. Di Paola, M. Zingales, Long-range cohesive interactions of non-local continuum faced by fractional calculus, International Journal of Solids and Structures 45 (2008) 5642–5659.
[29] G. Cottone, M. Di Paola, M. Zingales, Fractional mechanical model for the dynamics of non-local continuum, Advanced Numerical Methods 11 (2009) 389–423.
[30] M. Di Paola, G. Inzerillo, M. Zingales, The finite element method for the mechanically based model of non-local continuum, International Journal for Numerical Methods in Engineering 86 (2011) 1558–1576.
[31] G. Borino, M. Di Paola, M. Zingales, A non-local model of fractional heat conduction in rigid bodies, European Physical Journal Special Topics 193 (2011) 173–184.
[32] M. Mongiovì, M. Zingales, On fractional order thermodynamics, Journal of Physics A: Mathematical and Theoretical (2014) (submitted for publication).
[33] M. Di Paola, M. Zingales, Exact mechanical models of fractional hereditary materials, Journal of Rheology 55 (2012) 983–1004.
[34] M. Di Paola, F.P. Pinnola, M. Zingales, A discrete mechanical model of fractional hereditary materials, Meccanica: An International Journal of Theoretical and Applied Mechanics (2012). http://dx.doi.org/10.1007/s11012-012-9685-4.
[35] R.L. Bagley, P.J. Torvik, Fractional calculus—a different approach to the analysis of viscoelastically damped structures, AIAA Journal 21 (1983) 741–748.
[36] R.L. Bagley, P.J. Torvik, Fractional calculus in the transient analysis of viscoelastically damped structures, AIAA Journal 23 (1985) 918–925.
[37] H. Schiessel, R. Metzeler, A. Blumen, T.F. Nonnenmacher, Generalized viscoelastic models: their fractional equations with solutions, Journal of Physics A: Mathematical and General 28 (1995) 6567–6584.
[38] N. Heymans, J.C. Bauwens, Fractal rheological models and fractional differential equations for viscoelastic behavior, Rheologica Acta 33 (1994) 210–219.
[39] W. Flügge, Viscoelasticity, Blaisdell Publishing Company, Waltham, 1967.
[40] L.E. Suarez, A. Shokooh, Response of systems with damping materials modeled using fractional calculus, Applied Mechanics Reviews 48 (1995) S118–S126.
[41] Yu.A. Rossikhin, M.V. Shitnikova, A new method for solving dynamic problems of fractional derivative viscoelasticity, International Journal of Engineering Science 39 (2001) 149–176.